Available online at www.sciencedirect.com

ScienceDirect

Ceramics International 36 (2010) 969–977

CERAMICS INTERNATIONAL

www.elsevier.com/locate/ceramint

Synthesis of manganese ferrite from non-standard raw materials using ceramic technique

Y.M.Z. Ahmed *

Central Metallurgical Research and Development Institute (CMRDI), P.O. Box: 87 Helwan, Cairo, Egypt

Received 27 July 2009; received in revised form 30 September 2009; accepted 1 November 2009
Available online 2 December 2009

Abstract

Manganese ferrite spinel has been synthesized by using mill scale and fines of manganese ore sinter as sources of iron oxide and manganese oxide, respectively. The magnetic and physico-mechanical properties of the produced sample are largely dependent not only on the sintering condition but also on the Mn:Fe mole ratio. The effect of silica (which is one of the constituents of the fines of manganese ore sinter) on the properties of the sintered samples is investigated. The results show that a single phase of manganese ferrite spinel with weak magnetic properties is obtained in a sample containing a Mn:Fe mole ratio of 1.4:2 and sintered at 1300 °C for 2 h. On the other hand, a maximum saturation magnetization (62 emu/g) with reasonable physico-mechanical properties is obtained for a sample containing a Mn:Fe mole ratio of 1.3:2 and sintered at the same sintering conditions.

Keywords: C. Magnetic properties; Manganese ferrite; Physical properties; Compressive strength

1. Introduction

Discovering how to utilize waste reduction and resources, recycling programs effectively have become a priority in the last two decades. The increasing production of industrial solid waste has reached the point at which changes must be made, including the implementation of waste minimization strategies. It is becoming increasingly evident that a waste management program, and especially selection of the treatment and disposal facilities of waste residues, should involve economic as well as social aspects. Mill scale and fines of manganese ore sinter represent extensive examples of these waste materials.

Mill scale is considered as a valuable secondary raw material as a result of its high iron content, low impurities and stable chemical composition. This material is produced in huge quantities in steel making plants during the heating and subsequent rolling of steel slabs. Its specific production is about 35–40 kg/ton of hot rolled product. Thus, for a million ton-a-year steel plant, 35,000–40,000 tons of mill scale is produced. This amount of mill scale contains about 25,000–30,000 tons iron. On the other hand, large amounts of manganese ore sinter fines were accumulated in Ferromanganese Company (in Egypt). These fines are produced during shipping, handling and transportation of imported manganese ore sinter from different countries for ferromanganese production. Its amount is varied from year to another depending on the economic aspects of the factory. In general thousand of tons of this material are annually produced. However, this partially reduced ore is also considered as a valuable secondary raw material according to its high manganese content. Accordingly, these materials could be an excellent candidate in synthesizing a variety of both hard and soft ferrites especially manganese ferrite spinel.

Magnetic spinel ferrites are of great interest in fundamental science, especially for addressing the fundamental relationship between magnetic properties and their crystal chemistry and structure [1,2]. They find extensive applications in microwave devices, radar, digital recording, ferrofluids, catalysis and magnetic refrigeration systems [3–5]. The general formula of the spinel ferrite is AB_2O_4, consisting of an almost perfect cubic closed packed oxygen arrangement, with the cations residing on tetrahedral and octahedral interstices. Manganese ferrite is a partial inverse spinel ferrite, where about 20% of the Mn^{2+} ions are on B sites (or

---

* Tel.: +20 2 25516462; fax: +20 2 25010639.
E-mail address: ahmedymz@hotmail.com.

0272-8842/$36.00 © 2009 Elsevier Ltd and Techna Group S.r.l. All rights reserved.
doi:10.1016/j.ceramint.2009.11.020

octahedral coordination sites) and the rest reside on the A sites (or tetrahedral coordination sites) [6]. The remaining A and B sites are occupied by Fe^{3+} cations. Since the cation type, occupancy, and valence determine the magnetic and electronic properties of this important class of materials, there have been many studies attempting to explain the role of magnetic ions' distribution [7]. The previous studies reveal that at high temperatures (>900 °C) magnetic ions or non magnetic substitutions have sufficient energy to migrate from site to site. Thus the growth of a spinel by conventional means usually occurs above 900 °C.

To obtain manganese ferrite powders, several synthetic methods have been developed. Significant examples have used co-precipitated hydroxides [8,9], oxalates [10,11], citrates [12], micelle and reverse micelle [13,14–16], as well as combustion [17]. Although these processes permit one to obtain high purity manganese ferrite, these processes suffer from the high costs of the reactant used and the relative complexity of the technological procedures. However, ceramic method has been regarded as the most economical and widely used process in ferrite synthesis. In commercial technologies where ferrites are used as a rule, materials of high density are required. Thus, manganese ferrites are often prepared from finely ground and highly reactive precursor powders that, at high temperatures, are densified by sintering through solid-state reactions.

Meanwhile, using secondary resources or waste materials can bring a higher output of ferrite at lower cost and make a break-through in raw materials as well as technology. So it can be considered as an economically valuable and environmental-friendly process. To the best of my knowledge no reports regarding the use of non-standard raw materials for in situ formation of densified manganese ferrite has been reported so far. Here, a ceramic method was applied to investigate the effect of both sintering temperature and Mn:Fe mole ratio on the phase formation during sintering as well as the physical, mechanical and magnetic properties of the sintered sample using secondary resources. Meanwhile, owing to the high silica content of manganese ore sinter fines, extensive study on the effect of this silica content on the various properties of the produced sinter sample is conducted.

2. Experimental procedure

A mill scale sample was obtained from the Egyptian Iron and Steel Company. While the manganese ore sinter fines were delivered by the Sinai Ferro-manganese Company located at Sinai, Egypt. The total chemical composition of both materials is shown in Table 1. Both materials were finely ground to a mean particle size of 0.074 mm. Different batches of both materials with various Mn:Fe mole ratios were thoroughly mixed. The mixed samples were pressed into compacts of nominal diameter 13 and 18 mm height using a uniaxial press machine. The green compacts produced were dried at 105 °C for 24 h, then treated at different temperatures from 900 to 1300 °C for 2 h in a muffle furnace (model Nobertherm program controller C19).

Table 1
Chemical composition of non-standard raw materials.

Composition (%)	Fines of imported manganese ore sinter	Mill scale
Mn	42.0	–
MnO_2	65.10	–
MnO	1.03	–
Fe_{total}	4.0	74.2
Fe_{metal}	–	4
FeO	–	63.9
Fe_2O_3	8.72	29.3
P	0.09	–
SiO_2	17.10	0.36
Al_2O_3	6.00	0.14
K_2O	0.30	–
CaO	1.00	0.18
MgO	0.25	0.13
S	–	0.022
C	–	0.65

Table 2
Chemical composition of final product produced from sample containing different Mn:Fe mole ratios.

Composition (%)	Mn:Fe mole ratio			
	1:2	1.1:2	1.3:2	1.4:2
Mn_{total}	20.96	22.13	24.24	25.2
MnO	27.05	28.56	31.29	32.53
Fe_{total}	41.93	40.23	37.3	35.99
Fe_2O_3	59.9	57.47	53.28	51.41
P	0.043	0.045	0.05	0.05
SiO_2	8.36	8.76	9.45	9.76
Al_2O_3	2.94	3.08	3.32	3.43
K_2O	0.14	0.15	0.16	0.17
CaO	0.58	0.59	0.62	0.64
MgO	0.19	0.19	0.2	0.2

The chemical composition of the final products produced from sample containing different Mn:Fe mole ratios is shown in Table 2.

The bulk density and apparent porosity of the sintered compacts were evaluated using the Archimedes method. The compressive strength of the sintered compacts was carried out

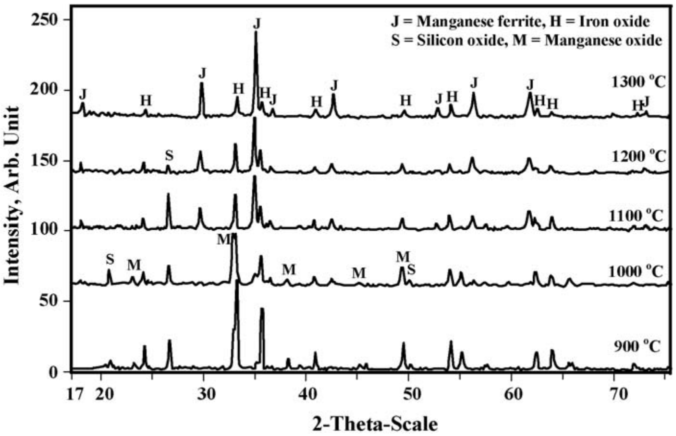

Fig. 1. XRD patterns of a sample containing a Mn:Fe mole ratio of 1:2 and sintered at different temperatures.

at ambient temperature using a universal test machine having a strain rate of $9.26 \times 10^{-4}\ s^{-1}$.

The different phases formed during different sintering temperatures were identified by X-ray diffraction (XRD) technique (PW 1730) with nickel-filtered Cu radiation ($\lambda = 1.5$ Å) at 40 kV and 30 mA. On the other hand, the microstructural changes accompanying the heat treatment of the compacted mixture were examined by a scanning electron microscope (JEOL-JSM-5410) equipped with energy dispersive X-ray spectrometer unit.

The magnetic properties of the samples were studied at room temperature in a maximum applied field of 15 kOe using a vibrating sample magnetometer model (VSM-9600M -1, USA).

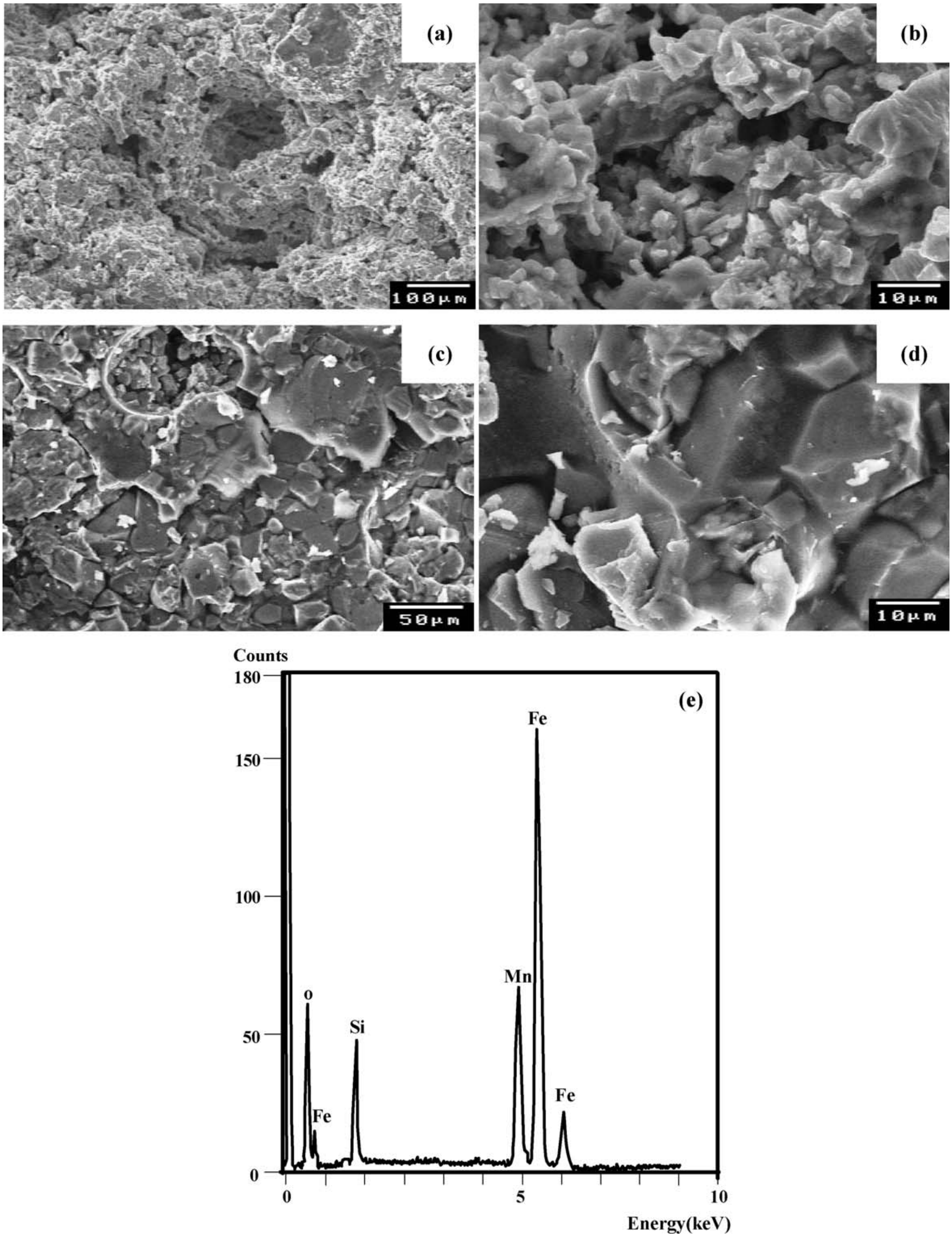

Fig. 2. SEM micrographs for samples sintered at different temperatures and containing a Mn:Fe mole ratio of 1:2. (a and b) Low and high magnification of sample fired at 1100 °C. (c and d) Low and high magnification of sample fired at 1300 °C. (e) EDX analysis for sample sintered at 1300 °C.

3. Results and discussion

3.1. Effect of sintering temperature

The X-ray diffraction patterns for samples containing a Mn:Fe mole ratio of 1:2 and sintered at different temperatures are shown in Fig. 1. The detection of many phases (iron oxide (JCPDS # 73-2234), manganese oxide (JCPDS # 73-1826), silica (JCPDS # 05-0490) and traces of manganese ferrite spinel (JCPDS # 74-2403)) at 900 °C indicates the incomplete reaction between the mill scale and the fines of manganese sinter for ferrite formation. With an increase in the sintering temperatures it is clearly noticed that the amount of spinel is increased at the expense of decreasing both of the iron oxide and manganese oxide contents. At 1100 °C the peaks characteristics for manganese oxide have completely disappeared and the spinel phase became the main phase. With a further increase in temperature to 1200 and 1300 °C the peak intensity characteristics for the spinel phase have been greatly increased beside the presence of a significant amount of iron oxide. These results indicated that manganese ferrite formation is largely dependent on the sintering temperature. The formation of manganese ferrite is believed to proceed via first transformation of Mn^{3+} into Mn^{2+}. This transformation is commenced at temperature above 900 °C [18]. While in practice the full formation of single phase manganese ferrite from the starting precursors (using ceramic method) is not observed until above 1200 °C. These facts interpret the traces of ferrite formed at 900 °C with the incomplete formation of single phase ferrite till 1200 °C. Meanwhile, the incomplete formation of single phase ferrite even at much higher temperature (1300 °C) could be attributed to the presence of silica in the starting precursors. It is worthy of mention that the peak characteristics for quartz were present in the sample till 1100 °C. Beyond this temperature the major peak intensity for quartz (at 2θ of 26.65) sharply decreased till it completely disappeared at 1300 °C. It is well known that when the temperature of a partially reduced manganese ore is increased above 1100 °C, liquid manganese silicate is formed, which is fluxed by alumina and basic (particularly alkali) oxides. Fluxing by alumina lowered the liquid temperatures of MnO–SiO_2 eutectic from 1250 to 1140 °C [19]. This behavior is responsible for consuming some amounts of MnO (necessary for complete formation of single spinel phase) via its side reaction with SiO_2 for liquid manganese silicate formation. Accordingly, the sample sintered at 1300 °C still contained a considerable amount of iron oxide (as shown in Fig. 1). Scanning electron micrographs (SEM) of samples sintered at 1100 and 1300 °C with EDX analysis confirmed this observation. Both the low and high magnification images (Fig. 2a and b) for the sample fired at 1100 °C showed microstructures with fairly small grains and open porosity. This indicates that these sintering conditions (1100 °C for 2 h) are insufficient for the completion of the solid–solid reaction between the different constituents. On the other hand, the low and high magnification images (Fig. 2c and d) for the sample sintered at 1300 °C clearly indicate the formation of large grains surrounded by a liquid phase. Kurtz and Carpary et al. [20] developed a theory to describe particle growth in ferromagnetic ceramics. They showed that the particle growth depends on both the duration of the sintering process and the temperature used. In general, the particle size increases monotonically with longer annealing times and the use of higher temperatures. Fig. 2d illustrates that abnormal grain growth occurred with an increase in the sintering temperature from 1100 to 1300 °C. The enhancement in grain growth via liquid phase sintering is a result of the liquid manganese silicate formation. Fig. 2e shows the elemental analysis using an energy dispersive X-ray spectrometer (EDX) for the sample sintered at 1300 °C. It reveals that the sample contains a considerable

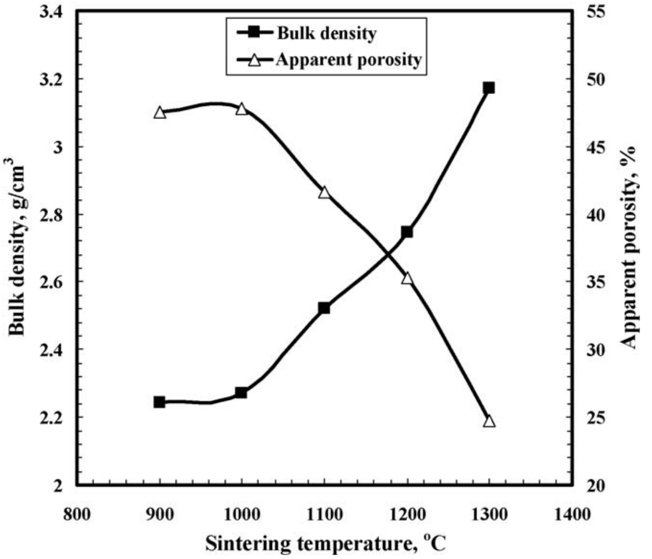

Fig. 3. Effect of sintering temperature on both bulk density and apparent porosity of sintered samples.

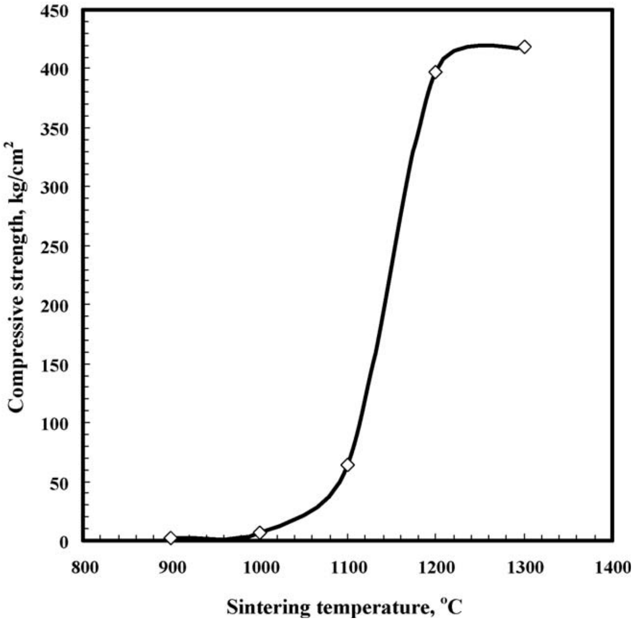

Fig. 4. Effect of sintering temperature on the compressive strength of sintered samples.

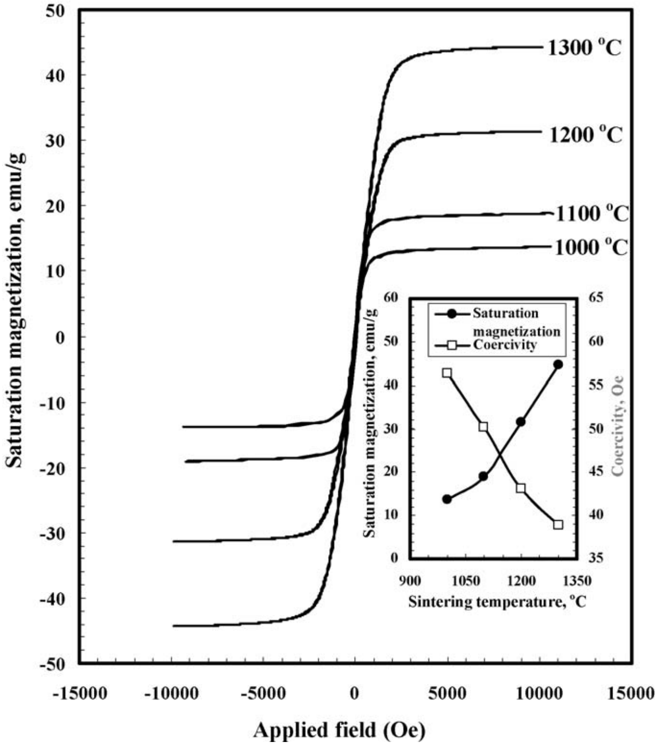

Fig. 5. M–H hysteresis loop of manganese ferrite synthesized at different sintering temperatures. The inset is the relationship between magnetic properties and sintering temperature.

amount of SiO_2 which is not observed in the XRD pattern of this sample. This confirms that silica is in the form of manganese silicate glass phase.

Fig. 3 shows the effect of sintering temperature on both the bulk density and apparent porosity of the sintered samples. It indicates that with an increase in the sintering temperature, the bulk density is largely increased while the apparent porosity is sharply decreased. This behavior is attributed to the enhancement of solid–solid reactions of the different constituents with an increase in the temperature. On the other hand, the compressive strength of sintered samples is found to be sharply increased with the sintering temperature up to 1200 °C then it only slightly increased at 1300 °C as shown in Fig. 4. The sharp increase in the compressive strength is due to the sharp decrease in the sample porosity. However, it was expected that with a further increase in temperature beyond 1200 °C the compressive strength should be sharply increased in a manner similar to the sample porosity (as shown in Fig. 3). The slight increase in compressive strength at 1300 °C could be attributed to the formation of a glassy phase of manganese silicate which weakens the structure. The intergranular glass phase causes a weakening of the microstructure when exposed to mechanical stress [21].

The hysteresis loops of the sintered samples are shown in Fig. 5, while the inset graphs represent the relationship between sintering temperature and both saturation magnetization and coercivity. It is noticed that increasing the sintering temperature

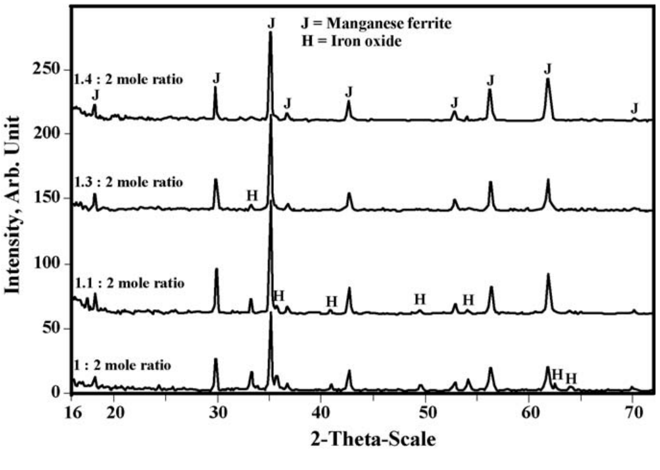

Fig. 6. XRD patterns of samples sintered at 1300 °C and containing different Mn:Fe mole ratios.

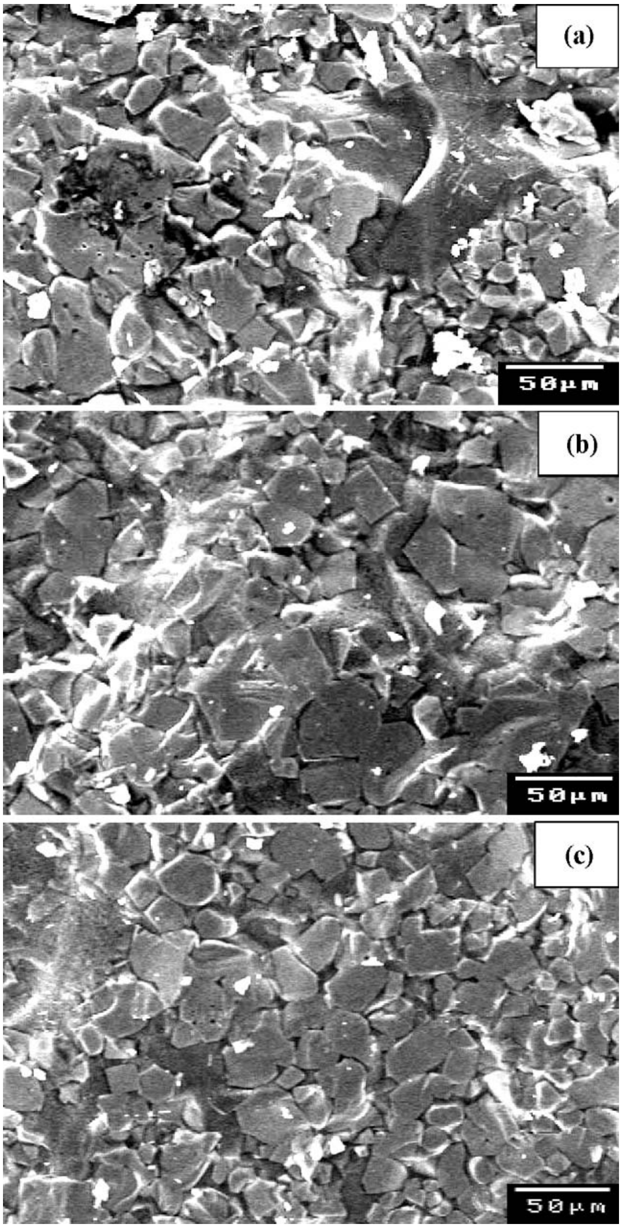

Fig. 7. Low magnification SEM micrographs for samples sintered at 1300 °C and containing different Mn:Fe mole ratios. (a) Mn:Fe mole ratio is 1.1:2. (b) Mn:Fe mole ratio is 1.3:2. (c) Mn:Fe mole ratio is 1.4:2.

leads to an increase in the saturation magnetization with a decrease in the coercivity. The magnetic property of samples is highly dependent on the microstructural changes brought about by the sintering process [22]. Saturation magnetization is directly proportional with both the sample density and grain size while the coercivity is inversely proportional with the sample grain size [23]. The increase in saturation magnetization with sintering temperature is attributed to the increase in the spinel phase formation as well as the sharp increase in sample bulk density. The change in saturation magnetization is found to be almost similar to the change in sample density with an increase in the sintering temperature. However, an increase in the sintering temperature is responsible for the growth in the spinel phase formed as dictated from the micrograph (Fig. 2). This increase in the grain size is the main reason for a decrease in the coercivity with an increase in the sintering temperature [22]. Also increasing the grain size in the sintered samples positively affected the saturation magnetization.

3.2. Effect of the Mn:Fe mole ratio

The previous investigation indicates that it is difficult to obtain a single phase spinel by using a Mn:Fe mole ratio of 2:1 as a result of consuming a part of MnO in a side reaction. Accordingly, a study concerning the effect of different Mn:Fe mole ratios on the phase formation as well as the physical, mechanical and magnetic properties of samples sintered at 1300 °C for 2 h was conducted.

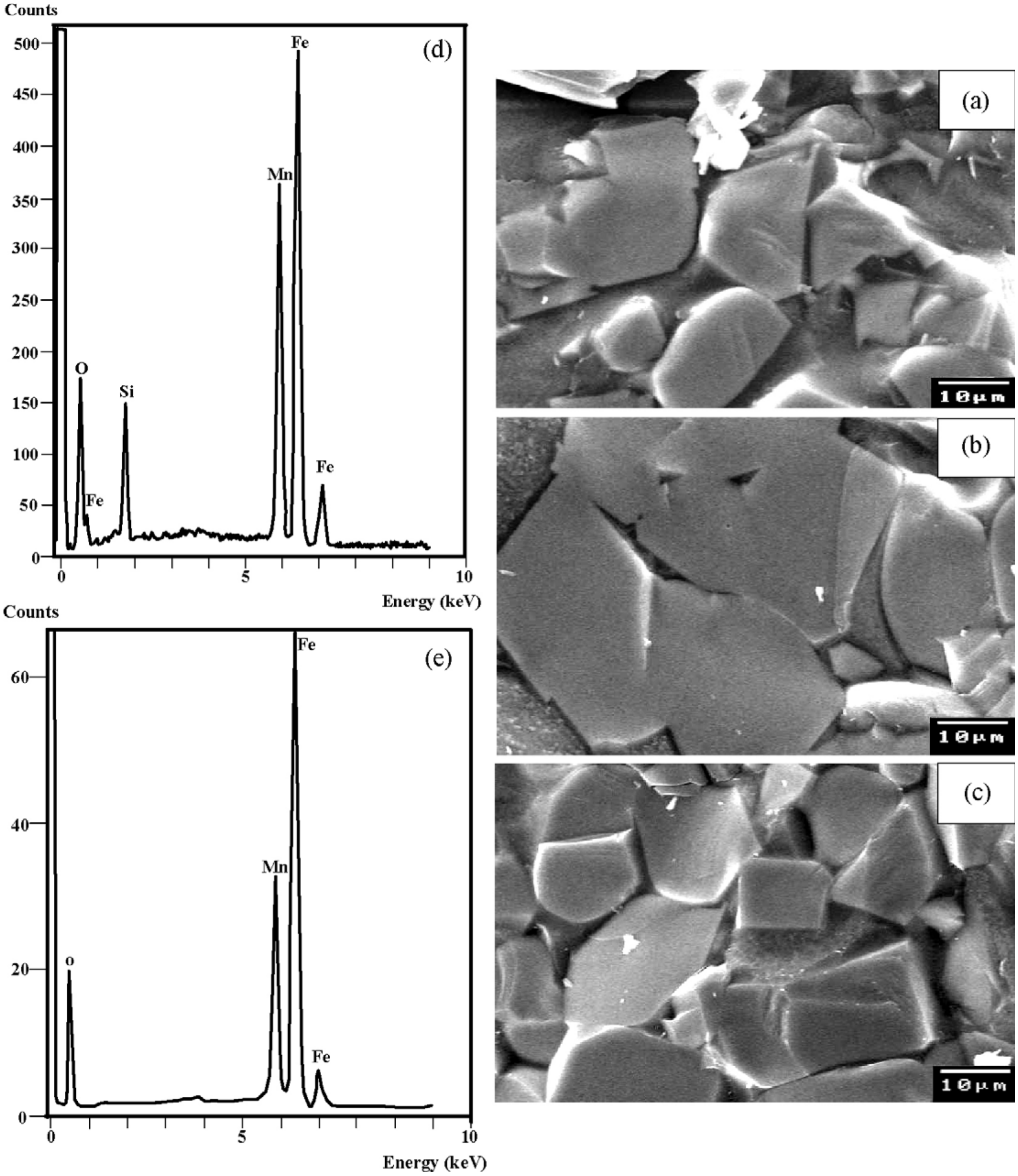

Fig. 8. High magnification SEM micrographs for samples sintered at 1300 °C and containing different Mn:Fe mole ratios: (a) Mn:Fe mole ratio is 1.1:2. (b) Mn:Fe mole ratio is 1.3:2. (c) Mn:Fe mole ratio is 1.4:2. (d) EDX analysis of sample containing a Mn:Fe mole ratio of 1.4:2. (e) EDX analysis for the ferrite grain (sample fired at 1300 °C).

Fig. 6 shows the X-ray diffraction patterns for sintered samples containing different Mn:Fe mole ratios. It is noticed that with an increase in the Mn:Fe mole ratio a continuous decrease in the iron oxide phase is clearly detected. At a Mn:Fe mole ratio of 1.4:2 a single phase of the Fd3m cubic spinel structure of manganese ferrite is obtained. This is extra evidence for the first finding that some part of the MnO is consumed in a side reaction with SiO_2 to form manganese silicate. Increasing the Mn mole ratio leads to an increase in the amount of MnO in the reaction media for completing the reaction with Fe_2O_3 present in the sample to produce manganese ferrite. It is important to mention that increasing the Mn mole ratio is also responsible for introducing more silica into the reaction environment. This is the main reason for retardation in the formation of the spinel single phase until a Mn:Fe mole ratio of 1.4:2.

SEM micrographs for sintered samples containing different Mn:Fe mole ratios at lower and higher magnifications are shown in Figs. 7 and 8, respectively. Figs. 7a, b and 8a, b reveal that with an increasing mole ratio a large enhancement in the grain growth is clearly observed which is ascribed to liquid phase sintering [24] caused by the formation of manganese silicate glass. But at higher mole ratio (at 1.4:2) (Figs. 7c and 8c) the size of the grains is largely reduced. This behavior at highest mole ratio is understandable, as the excess of manganese silicate glass starts to segregate at the grain boundaries hindering the growth of the grain beyond a significant size. The EDX analysis for the whole surface of sample containing highest mole ratio (Fig. 8d) indicates the presence of significant amount of silica which is believed to be in the form of manganese silicate glass precipitated at the grain boundaries. On the other hand, the EDX analysis of the large ferrite spinel grains (Fig. 8e) indicates the absence of any impurities in the formed spinel structure. This confirms that all impurities of the starting material are directly precipitated at the grain boundaries without any inclusions on the ferrite structure.

Fig. 9 shows the effect of different mole ratio on the bulk density and apparent porosity of sintered samples. It is clear that with an increase in the Mn:Fe mole ratio the bulk density is sharply increased while the apparent porosity is largely decreased. The increase in the bulk density is due to the increase in the amount of liquid glassy phase in the sintered sample which consequently leads to a decrease in the apparent porosity. Also grain growth plays an important role in enhancing the sample density and reducing the apparent porosity. These two modes (grain growth and amount of liquid phase) easily explain the fluctuating behavior of the compressive strength with an increase in the Mn:Fe mole ratio shown in Fig. 10. It was found that firstly (at a 1.1:2 mole ratio) the compressive strength increased as a result of a decrease in the apparent porosity. At a 1.3:2 mole ratio the remarkable decrease in the compressive strength is due to the increase in the content of glassy phase which weakens the microstructure. Also the grain size contributes to change the compressive strength of the sintered samples. It is well known that a finer and homogeneous grain size is responsible for enhancing the mechanical properties of samples [25]. With a further increase in the mole ratio (to 1.4:2) the compressive strength was found to increase again. This behavior of the sample, e.g., containing the highest mole ratio was attributed to the formation of a much smaller grain size as a result of grain growth retardation. However, the compressive strength value of this sample is much less than the sample containing a 1.1:2 mole ratio and even from the sample containing a 1:2 mole ratio which is attributed to the formation of a large amount of the glassy phase.

The effect of different Mn:Fe mole ratios on the magnetic properties of sintered samples is shown in Fig. 11. It can be seen

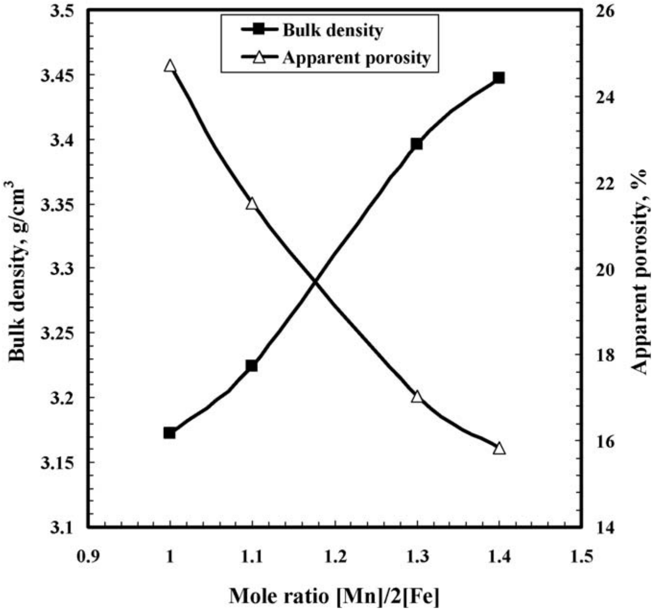

Fig. 9. Effect of different Mn mole ratios on both the density and the apparent porosity of samples sintered at 1300 °C.

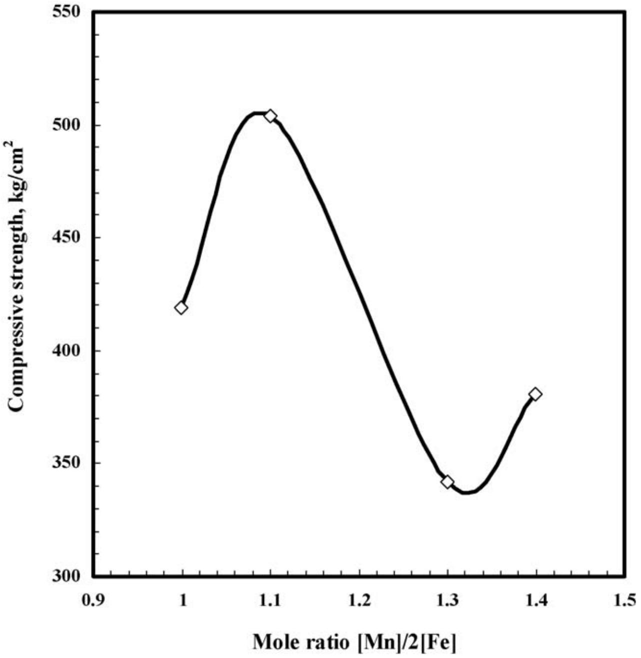

Fig. 10. Effect of different Mn mole ratios on the compressive strength of sample sintered at 1300 °C.

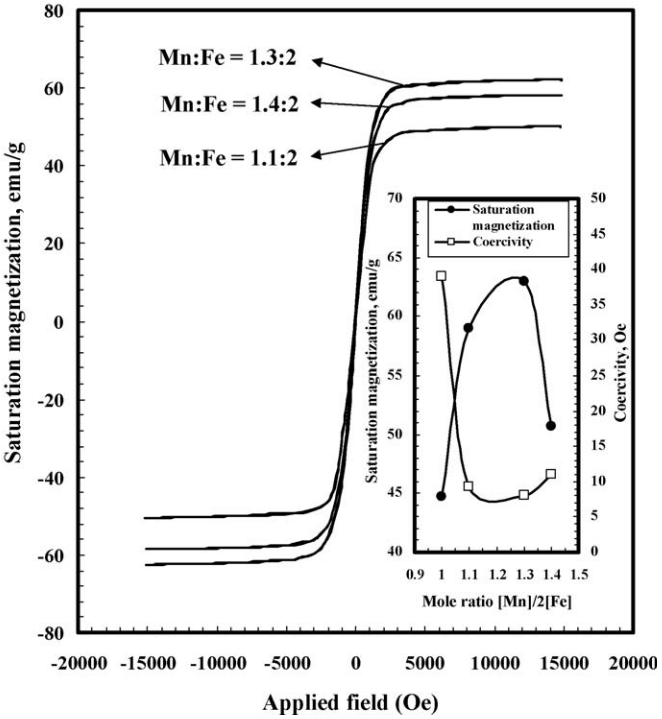

Fig. 11. M–H hysteresis loop of manganese ferrite synthesized from samples containing different Mn mole ratio and sintered at 1300 °C. The inset is the relationship between magnetic properties and [Mn]/2[Fe] mole ratios.

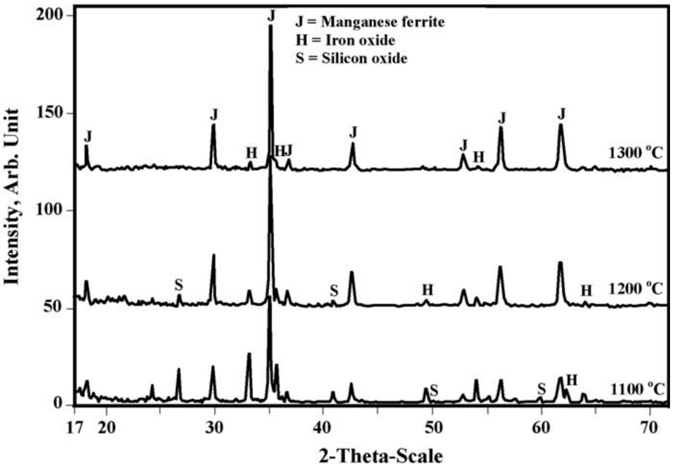

Fig. 12. XRD patterns of samples sintered at different temperature and containing a Mn:Fe mole ratio of 1.3:2.

Table 3
Effect of different sintering temperature on the physical properties of samples containing a Mn:Fe mole ratio of 1.3:2.

Physical properties	Sintering temperature (°C)		
	1100	1200	1300
Density (g/cm^3)	2.5	2.8	3.4
Apparent porosity (%)	42.5	33.9	17.0
Compressive strength (kg/cm^2)	149.3	322.2	341.8

that the saturation magnetization is largely increased with an increase in the mole ratio until it reaches a maximum at a 1.3:2 mole ratio and then it decreases thereafter, while coercivity shows the opposite trend. The highest saturation magnetization obtained at this mole ratio was found to be about 62 emu/g which is not far from the value reported for bulk manganese ferrite (80 emu/g) [26,27]. The increase in saturation magnetization as well as the decrease in the coercivity is attributed to the large increase in both the grain size and bulk density. Beyond a 1.3:2 mole ratio of Mn:Fe it was noticed that there was a sharp decrease in saturation magnetization with a slight increase in coercivity (the sample containing a Mn:Fe mole ratio of 1.4:2). This behavior is attributed to the retardation of grain growth with the formation of a smaller grain size as a result of the formation of a considerable amount of manganese silicate. It is worth mentioning that the saturation magnetization of this sample is much lower than that of the sample that even contained the Mn:Fe mole ratio of 1.1:2. However, not much difference in the grain size between these samples was noticed (Fig. 7). Taking into consideration that single spinel phase only was observed with this mole ratio. This behavior is attributed to the formation of high amount of manganese silicate surrounding the ferromagnetic manganese ferrite grains which weakens the magnetic properties of the sintered sample.

The effect of different sintering temperatures on the properties of samples possessing the highest magnetic properties was investigated. The XRD patterns for samples containing a Mn:Fe mole ratio of 1.3:2 and sintered at different temperatures for 2 h are shown in Fig. 12. It is noticed that the behavior of phase changes in these samples by varying the sintering temperature is similar to the sample containing the Mn:Fe mole ratio of 1:2 previously discussed. The only difference that could be elaborated from the patterns is a change in the intensity of the main peak characteristics for silica. Herein the peak intensity is much higher. This was expected as a result of an increase in the silica content in these samples. On the other hand it was found that with an increase in the sintering temperature the bulk density and consequently the compressive strength are increased while the apparent porosity is decreased as shown in Table 3.

4. Conclusion

Manganese ferrite spinel was successfully synthesized from non-standard raw materials using a ceramic method. The effects of both the sintering temperature and the Mn:Fe mole ratio on the properties of the sintered sample were investigated. A single phase of manganese ferrite was difficult to obtain with samples containing a Mn:Fe mole ratio of 1:2 even at higher sintering temperatures. A part of manganese oxide in the sample is consumed in a side reaction with silica present in the raw material to form a liquid phase manganese silicate. This liquid phase enhances the grain growth and consequently enhances the magnetic properties as well as the physical properties of the sintered sample. The highest saturation magnetization value, which is not far from the value of bulk manganese ferrite was obtained for a sample containing a Mn:Fe mole ratio of 1.3:2 and sintered at 1300 °C for 2 h.

References

[1] M.R. DeGuire, G. Kalonji, R.C. O'Handley, Cation distributions in rapidly solidified cobalt ferrite, J. Am. Ceram. Soc. 73 (10) (1990) 3002–3006.

[2] M.A. Willard, Y. Nakamura, E.D. Laughlin, E.M. McHenry, Magnetic properties of ordered and disordered spinel-phase ferrimagnets, J. Am. Ceram. Soc. 82 (12) (1999) 3342–3346.

[3] M.P. Horvath, Microwave application of soft ferrites, J. Magn. Magn. Mater. 215 (2000) 171–183.

[4] J.D. Adams, L.E. David, G.F. Dionne, E.F. Schloemann, S.N. Stitzer, Ferrite devices and materials, IEEE Trans. Microwave Theory Tech. 50 (2002) 721–737.

[5] Z.H. Zhou, J.M. Xue, J. Wang, $NiFe_2O_4$ nanoparticles formed in situ in silica matrix by mechanical activation, J. Appl. Phys. 91 (2002) 6015–6020.

[6] E.W. Gorter, Saturation magnetization and crystal chemistry of ferromagnetic oxides, Philips Res. Rep. 9 (1954) 295–320.

[7] J. Sakurai, T. Shinjo, Neutron diffraction of manganese ferrite prepared from aqueous solution, J. Phys. Soc. Jpn. 23 (1967) 1426–11426.

[8] V.M. Burojeanu, L. Fournes, A. Wattiaux, J. Etourneau, E. Segal, Cation distribution and magnetic properties of manganese ferrite powder prepared by coprecipitation from MnO_2 and $FeSO_4{\cdot}7H_2O$, Int. J. Inorg. Mater. 3 (2001) 525–529.

[9] Z.X. Tang, C.M. Sorensen, K.J. Klabunde, G.C. Hadjipanayis, Preparation of manganese ferrite fine particles from aqueous solution, J. Colloid Interface Sci. 146 (1991) 38–52.

[10] B. Gillot, M. Laarj, S. Kacim, Reactivity towards oxygen and cation distribution of manganese iron spinel $Mn_{3-x}Fe_xO_4$ ($0 \leq x \leq 3$) fine powders studied by thermogravimetry and IR spectroscopy, J. Mater. Chem. 7 (1997) 827–831.

[11] M. Bremer, S. Fischer, H. Langbein, W. Topelmann, H. Scheler, Investigation on the formation of manganese–zinc ferrites by thermal decomposition of solid solution oxalates, Thermochim. Acta 209 (1992) 323–330.

[12] N.S. Gajbhiye, G. Balaji, Synthesis, reactivity, and cations inversion studies of nanocrystalline $MnFe_2O_4$ particles, Thermochim. Acta 385 (2002) 143–151.

[13] R.D.K. Misra, S. Gubbala, A. Kale, W.F. Egelhoff Jr., A comparison of the magnetic characteristics of nanocrystalline nickel, zinc, and manganese ferrites synthesized by reverse micelle technique, Mater. Sci. Eng. B111 (2004) 164–174.

[14] C. Liu, B. Zou, J. Rondinone, Z.J. Zhang, Reverse micelle synthesis and characterization of superparamagnetic $MnFe_2O_4$ spinel ferrite nanocrystallites, J. Phys. Chem. B 104 (2000) 1141–1145.

[15] E.E. Carpenter, C.J. O'Connor, V.G. Harris, Atomic structure and magnetic properties of $MnFe_2O_4$ Nanoparticles produced by reverse micelle synthesis, J. Appl. Phys. 85 (8) (1999) 5175–5177.

[16] S. Sun, H. Zeng, B. Robinson, S. Raoux, P.M. Rice, S.X. Wang, G. Li, Monodisperse MFe_2O_4 (M = Fe, Co, Mn) nanoparticles, J. Am. Chem. Soc. 126 (2004) 273–279.

[17] Y. Li, J. Jiang, J. Zhao, X-ray diffraction and Mössbauer studies of phase transformation in manganese ferrite prepared by combustion synthesis method, Mater. Chem. Phys. 87 (2004) 91–95.

[18] F.J.C.M. Toolenaar, M.T.J. Van Lierop-Verhees, Reactive sintering of manganese ferrite, J. Mater. Sci. 24 (1989) 402–408.

[19] N. Anacleto, O. Ostrovski, S. Ganguly, Reduction of manganese ore by methane-containing gas, ISIJ Int. 44 (10) (2004) 1615–1622.

[20] S.K. Kurtz, F.M.A. Carpay, Microstructure and normal grain growth in metals and ceramics. Part I. Theory, J. Appl. Phys. 51 (1980) 5725–5744.

[21] H. Baumgartner, J. Dreikorn, R. Dreyer, L. Michalowsky, E. Pippel, J. Woltersdorf, Manganese–zinc-ferrites with improved magnetic and mechanical properties, J. Phys. IV France (1997) 67–69.

[22] R.S. Devan, Y. Ma, B.K. Chougule, Effective dielectric and magnetic properties of (Ni–Co–Cu)ferrite/BTO composites, Mater. Chem. Phys. 115 (2009) 263–268.

[23] D.B. Shekhar, A.J. Pattayil, Effect of sintering conditions and microstructure on the magnetostrictive properties of cobalt ferrite, J. Am. Ceram. Soc. 91 (2008) 1976–1980.

[24] M.F. Yan, D.W. Johnson Jr., Impurity-induced exaggerated grain growth in Mn–Zn ferrites, J. Am. Ceram. Soc. 61 (7–8) (2006) 342–349.

[25] E.M.M. Ewais, M.M. Hessien, A.A. El-Geassy, In-situ synthesis of magnetic Mn–Zn ferrite ceramic object by solid state reaction, J. Aust. Ceram. Soc. 44 (2008) 57–62.

[26] R. Tebble, D.J. Craik, Magnetic Materials, Wiley-Interscience, New York, 1969.

[27] R.D.K. Misra, S. Gubbala, A. Kale, W.F. Egelhoff Jr., A comparison of the magnetic characteristics of nanocrystalline nickel, zinc, and manganese ferrites synthesized by reverse micelle technique, Mater. Sci. Eng. B 111 (2004) 164–174.